Articles

The Electrocatalytic Reduction of Molecular Oxygen with a Co(II)-Glyoxal Bis(2-hydroxyanil) Complex Coated Electrode

Euh Duck Jeong, Mi Sook Won†, and Yoon Bo Shim*

Department of Chemistry, Pusan National University, Pusan 609-735, Korea
†Pusan Branch, Korea Basic Science Institute, Pusan 609-735, Korea
Received

The electrocatalytic reduction of molecular oxygen was investigated with a Co(II)-glyoxal bis(2-hydroxyanil) complex coated-glassy carbon (GC) electrode in aqueous media. The reduction of O_2 at the modified electrode was an irreversible and diffusion-controlled reaction. The complex coated-GC electrode demonstrated an excellent electrocatalytic effect for O_2 reduction in an acetate buffer solution of pH 3.2. The coated electrode made the O_2 reduction potential shift of 60-510 mV in a positive direction compared to the bare GC electrode depending on pH. The Co(II)-glyoxal bis(2-hydroxyanil) coated electrode converted about 51% of the O_2 to H_2O_2 *via* a two-electron reduction pathway, with the balance converted to H_2O.

Introduction

Electrocatalysis of molecular oxygen reduction has a significant impact on the development of fuel cells and in electroorganic reactions.[1,2] The metal complexes of phthalocyanine[3-7] and porphyrin[8-12] were studied intensively as catalysts of oxygen reduction. Catalytic oxygen reduction takes place *via* two or four electron transfer reactions producing H_2O_2 or H_2O. It goes through the formation of an adduct[13] or oxo-bridged complex[14,15] between the metal ions and molecular oxygen.

While there exist numerous studies on the metal complexes of phthalocyanines and porphyrins to electrochemically catalyze the oxygen reduction, limited findings for the electrocatalytic effect on the reduction of molecular oxygen using other metal complexes with organic ligands,[16-18] including Schiff base,[19] have been reported. Anson *et al.* studied electrocatalytic activity for the reduction of oxygen and H_2O_2 with Cu(II) complexes of phenanthroline derivatives[17] and 2,3-bis(2-pyridyl)pyrazine.[16] Like porphyrin and phthalocyanine ligands, quadridentate Schiff base ligands can form planar metal complexes. In addition, metal complexes of Schiff bases as synthetic oxygen carriers also react with molecular oxygen in its lower oxidation state in both solid and solution states.[20] The formation constant of the oxygenation reaction of several Co(II)-Schiff base complexes has been determined by the spectrophotometric method.[21,22]

In the present work, we examined the catalytic effect of a Co(II)-Schiff base complex, Co(II)-glyoxal bis(2-hydroxyanil) (Co(II)-GHA) on oxygen reduction, at various pH. The Schiff base, glyoxal bis(2-hydroxyanil) (GHA) was synthesized by the condensation of *o*-aminophenol with glyoxal.[23] The GHA forms complexes in weak alkaline media with Co (II), Zn(II), Cd(II), and also with the alkaline earth metal ions.[24] Of these complexes, a Co(II)-GHA complex may form an adduct with molecular oxygen. Based on this, we expected that the Co(II)-GHA complex would catalyze the electrochemical reduction of molecular oxygen. Thus, the electrocatalytic reduction of O_2 on the Co(II)-GHA coated electrode was studied with cyclic voltammetry, rotating disk electrode (RDE), and rotating ring disk electrode (RRDE) experiments in KNO_3 and various pH media.

Experimentals

Synthesis of Co(II)-GHA Complex. All aqueous solutions were prepared with doubly distilled deionized water (Millipore, Milli-Q™ Water System). The initial product of GHA synthesized with the condensation of *o*-aminophenol and glyoxal[23] was not the open-chain Schiff base but the isomeric bis-2-benzoxazolinyl. In the weak alkaline media, the ring structure, which was incapable of forming complexes, was rearranged to the open-chain form to be a true complexing ligand. A Co(II)-GHA complex was synthesized from the reaction between GHA and cobalt nitrate (Aldrich, 99%) by the following method: GHA was dissolved in methanol, then it was slowly added to KOH in methanol (GHA : KOH=1 : 2 mole ratio). This solution was added to an aqueous $Co(NO_3)_2 \cdot 6H_2O$ solution at 60 °C under a nitrogen atmosphere. The reaction solutions were slowly stirred, and then stored in the refrigerator for 24 hours. The purplish red Co(II)-GHA precipitates were obtained by the centrifugation of the stored solution and recrystallized with methanol. The pure precipitate was dried at room temperature for 24 hours at reduced pressure. A 0.1 M KNO_3 solution, acetate (pH 3-6) and ammonia (pH 7-9) buffer, and NaOH (pH 13) solutions were used as supporting electrolytes. All other reagents were extra pure grade and were used without further purification.

Apparatus and Electrochemical Measurement. All the electrochemical experiments were performed in a two-compartment cell with three electrodes. A glassy car-

*To whom correspondence should be addressed.

bon (GC) electrode (area=1.13 cm^2) was used as a working electrode. It was polished with 1-3 μm alumina-water slurries, then washed with distilled water and acetone, and dried before each experiment. A Pt spiral wire was used as a counter electrode. As reference electrodes, $Hg/HgSO_4$ (EG & G PAR) and Ag/AgCl (sat'd) electrodes were used in cyclic voltammetry (CV) and hydrodynamic experiments (rotating disk and rotating ring disk electrodes), respectively. To modify the GC working electrode, we dipped it into a 1.0 mM Co(II)-GHA ethanolic solution while stirring for 30 minutes. The CV and RRDE experiments were performed using a model AFRDE 5 Bi-potentiostat (Pine Instruments Co.) and the output signals were recorded with an X-Y recorder (Kipp and Zonnen Co., Model BD 90). The rotating electrodes were rotated with the EG & G PAR Model 636 Rotating-Disk Electrode System. The elemental analysis (C, H, and N) of Co(II)-GHA was performed with Vario EL elemental analyzer at Pusan branch of KBSI.

The CVs were recorded between 0.0 V and −0.8 V *vs.* $Hg/HgSO_4$. In the RRDE experiment, the disk electrode potential was swept from 0.0 V to −0.8 V *vs.* $Hg/HgSO_4$ at 10 mV/s while the ring electrode potential was fixed at 1.0 V *vs.* $Hg/HgSO_4$ during the cathodic sweep.

Results and Discussion

The structures of GHA (a) and Co(II)-GHA (b) are shown in Scheme 1. The composition of the Co(II)-GHA complex was identified by elemental analysis. The result of the elemental analysis of Co(II)-GHA was as follows: (Calc. (%): C=50.16, H=4.81, N=8.36; Found: C=50.93, H=4.62, N=8.27). These results coincide with the proposed complex[24] structure in Scheme 1. The structure of the Co(II)-GHA complex is similar to that of Co(II)-SALEN in that they both have a square planar geometry.[25] Co(II)-SALEN forms an adduct with molecular oxygen in its axial position with the central metal ion.[21] This suggests that the Co(II)-GHA complex may also react with molecular oxygen to form an adduct.

To demonstrate that the adsorbed Co(II)-GHA complex catalyzes the reduction of molecular oxygen, cyclic voltammograms were recorded at bare and modified GC electrodes in an O_2 saturated 0.1 M KNO_3 solution (See Figure 1). The O_2 reduction potential at the bare GCE was −0.79 V, while that at the Co(II)-GHA complex coated electrode was −0.67 V. This shows that the Co(II)-GHA layer on the electrode catalyzed the oxygen reduction in a 0.1 M KNO_3 solution, shifting the potential value positively by 120 mV to −0.67 V. The reduction potential of O_2 at the electrode coated only with the ligand GHA was −0.85 V, which shifted in the negative direction compared to that at the bare GCE. This indicates that the GHA coated electrode has no catalytic activity. All the electrocatalytic reduction processes of molecular oxygen were irreversible in all pH ranges.

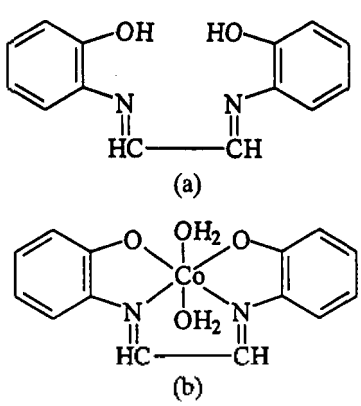

Scheme 1. Schematic structures of (a) GHA and (b) Co(II)-GHA complex.

To determine kinetic parameters for the reduction of O_2 on the bare and the Co(II)-GHA complex coated electrodes, CVs were recorded at various scan rates in an O_2 saturated 0.1 M KNO_3 solution. The peak currents were directly proportional to the square root of the scan rate at both electrodes, as shown in Figure 2. The linear correlation of i_p *vs.* $\nu^{1/2}$ indicates that the electrocatalysis of the O_2 reduction was under the control of a diffusion process.

The following equations (1) and (2), give the relationship of $(E_p\text{-}E^{o'})$ with $(\nu^{1/2})$ for a totally irreversible wave.[26]

$$E_p = E^{o'} - RT/\alpha n_a F[0.780 + ln(^*D_o^{1/2}/k_o) + ln(\alpha n_a F\nu/RT)^{1/2}] \quad (1)$$

$$E_p - E^{o'} = -RT/\alpha n_a F[0.780 + ln(^*D_o^{1/2}/k_o)] - ln(\alpha n_a F/RT)^{1/2} - RT/\alpha n_a F[ln(\nu^{1/2})] \quad (2)$$

where k_o is the exchange rate constant (cm/sec) and $E^{o'}$ is the formal potential of oxygen reduction. To calculate αn_a and k_o from the above equations, the $(E_p\text{-}E^{o'})$ values were plotted respective to $\ln(\nu^{1/2})$. Figure 3 shows the $(E_p\text{-}E^{o'})$ *vs.* $\ln(\nu^{1/2})$ plots from the CV data for the reduction of O_2 on (a) the bare and (b) Co(II)-GHA coated GCEs. The plot of $(E_p\text{-}E^{o'})$ *vs.* $\ln(\nu^{1/2})$ was linear with a slope of αn_a, and the k_o value was calculated from the intercept of this plot. The αn_a values were 0.66 and 0.42 on the bare and Co(II)-GHA coated GCEs, respectively. The exchange rate constant, k_o, calculated using the diffusion coefficient of O_2 (D_0=1.90×10^{-5} (cm^2/sec))[27] were 1.27×10^{-7} (cm/sec) for the Co(II)-GHA coated electrode and 1.58×10^{-11} (cm/sec) for the

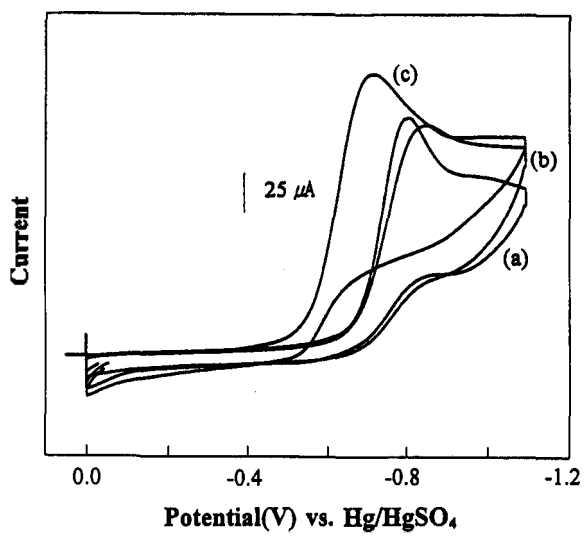

Figure 1. Cyclic voltammograms (scan rate: 50 mV/sec) of oxygen reduction in O_2 saturated 1 M KNO_3 solution: (a) the bare GC electrode, (b) the same electrode coated with GHA, and (c) coated with Co(II)-GHA.

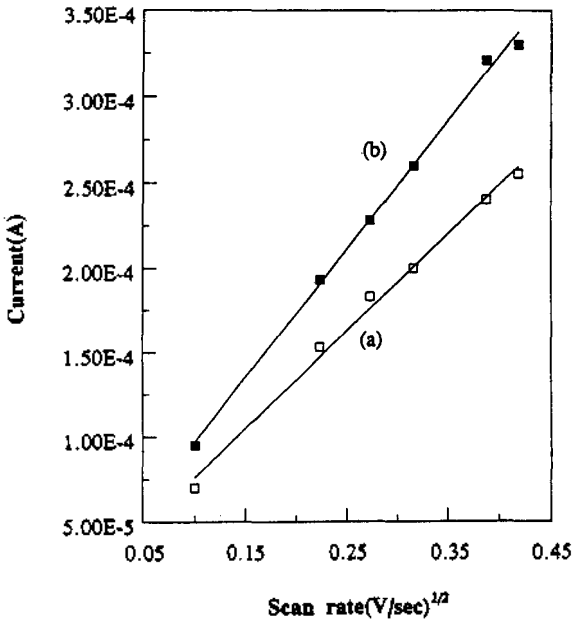

Figure 2. The oxygen reduction peak current as a function of the square root of scan rate in O_2-saturated 0.1 M KNO_3 solution: (a) the bare GC electrode and (b) Co(II)-GHA coated electrode.

bare GCE. The result shows that the exchange rate constant increased by about four orders of magnitude at the Co(II)-GHA coated electrode compared to that at the bare GCE.

To characterize the pH dependency of the potential of the molecular oxygen reduction, CVs were recorded for the Co (II)-GHA coated and bare electrodes over the range of pH 3.2 to 13.0. CVs at the bare GCE in (a) N_2-saturated and (b) O_2-saturated solutions, and the Co(II)-GHA coated electrode (c) in the O_2-saturated solution at pH 3.2 are shown in Figure 4(A). At pH 3.2, the reduction potential of molecular oxygen was -1.16 V for the bare GCE and -0.65 V for the Co(II)-GHA coated GCE. The Co(II)-GHA coated electrode shifted the potential of O_2 reduction positively by about 510 mV compared to that at the bare GCE. This result showed an excellent catalytic effect of the Co(II)-GHA coated electrode. We plotted the reduction peak potential (E_p) *vs.* pH with the bare GCE, the Co(II)-GHA coated electrode, and the GHA only coated electrode. The results in given pH media are shown in Figure 4(B). The potential shifts of the oxygen reduction were more effective in the acidic than the basic medium at the Co(II)-GHA coated electrode. Furthermore, the O_2 reduction potentials at bare, GHA coated, and Co(II)-GHA coated GC electrodes were almost the same at the higher pH values (pH > 9.0). It is well known that metal complexes of Schiff bases easily form an oxygenate complex:[20-22] in polarographic studies, the reduction of the oxygenated Schiff-base complex of CoSALEN-O_2 occurred at -0.63 V *vs.* Ag/AgCl in 0.1 M TEAP (tetraethylammonium perchlorate)-pyridine.[28] The E_p of the O_2 catalytic wave of Co(II)-GHA coated electrode was pH dependent with a slope of 60.9 mV/pH between pH 5.8 and 9.0. This result coincides with previous results for the reduction of O_2 using Fe-TSP (tetrasulfonate phthalocyanines),[3] Co-TSP (tetrapyridylporphyrine)[9] and Cu(II)-DPP(2,3-bis(2-

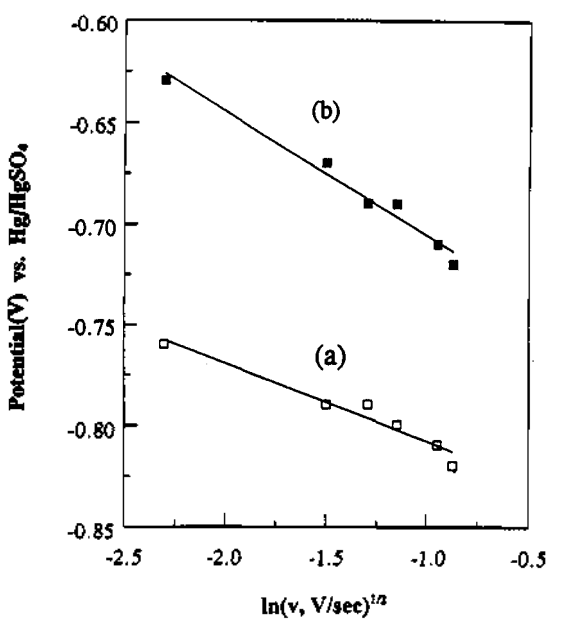

Figure 3. The oxygen reduction peak potential as a function of the $\ln(v^{1/2})$ in 0.1 M KNO_3 solution saturated with O_2: (a) the bare glassy carbon electrode and (b) Co(II)-GHA coated electrode.

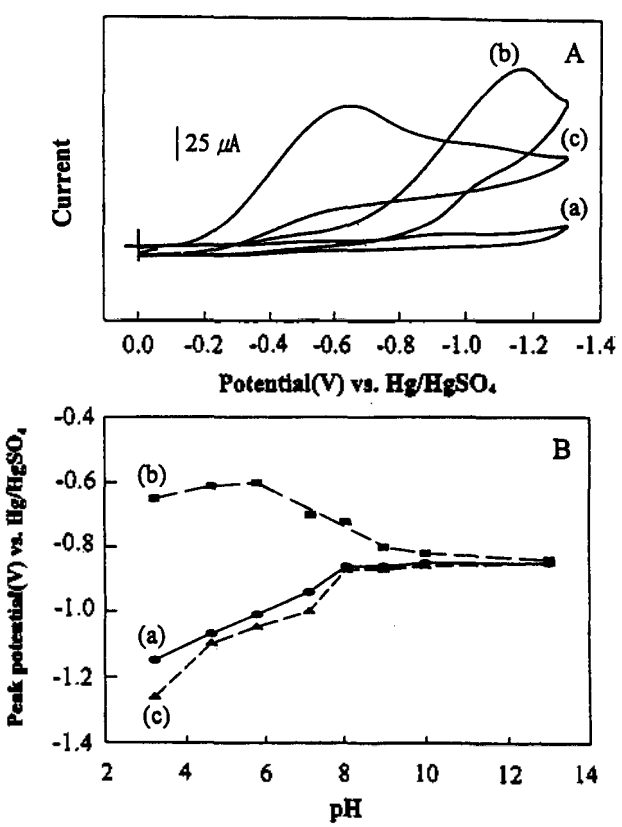

Figure 4. (A) Cyclic voltammograms (scan rate; 50 mV/sec) of oxygen reduction for the electrodes in a pH 3.2 acetate buffer solution. ((a) N_2-saturated solution with the bare GC electrode, (b) O_2-saturated solution with the bare GC electrode and (c) Co(II)-GHA coated electrode). (B) The oxygen reduction peak potential as a function of the pH of the solution. ((a) the bare GC electrode, (b) Co(II)-GHA coated electrode, and (c) the GHA coated electrode).

pyridyl) pyrazine).[16] The largest potential difference took place at pH 3.2. The reason for this result is presently uncertain.

In the acidic medium (pH<5.8), the magnitude of the O_2 reduction current at the Co(II)-GHA coated electrode was smaller than that at the bare GCE. In the higher pH range, the reduction current of O_2 at the Co(II)-GHA coated electrode was larger than that at the bare GCE. The effect of the reduction peak current on film thickness was investigated in a basic solution. On varying the film thickness of Co(II)-GHA, there are no apparent changes of the peak current. This indicates that the overall rate of catalytic reduction of oxygen may not be a diffusion-like charge propagation of O_2[29] in which the magnitude of the current is larger as the film thickness increases. Another possible explanation is that the high current in a basic solution may be achieved due to a superoxide easily formed.

The cyclic voltammograms were recorded at electrodes prepared at different coating times (5-30 min) in different concentrations of the Co(II)-GHA (0.1-1 mM). The magnitude of the reduction potential shift and the reduction current did not change with the different coating times and concentrations of the Co(II)-GHA complex in a 0.1 M KNO_3 solution. This indicates that only a monolayer of Co(II)-GHA on the electrode surface would be enough for catalytic activity. A study of the kinetics and the overall mechanisms of the catalytic reaction is important in the evaluation of the effectiveness of a catalyst of the O_2 reduction. This type of study can be carried out by the hydrodynamic method. Thus, the catalyzed reduction of oxygen was also examined with an RDE coated with Co(II)-GHA. As shown in Figure 5, the Levich plot was nonlinear as shown in other experiments for a catalyzed reduction reaction of O_2 in which a current limiting chemical reaction precedes the electron transfer.

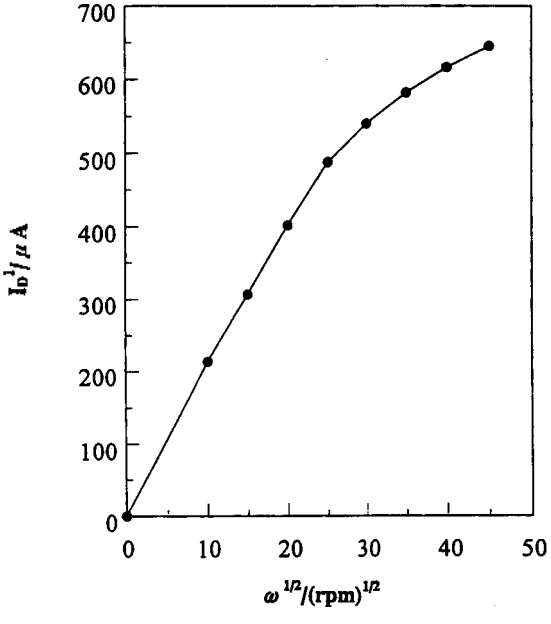

Figure 5. Levich plot of the I_D *vs.* $\omega^{1/2}$ for reduction of O_2 with the Co(II)-GHA coated electrode in an O_2-saturated 0.1 M KNO_3 solution. The disk electrode potential was swept from 0.0 V to −0.8 V *vs.* $Hg/HgSO_4$ at 10 mV/s.

The Koutecky-Levich plot[30] can be interpreted by the following equation (3);

$$1/i_{lim} = 1/i_k + 1/0.62nFAD^{2/3}\nu^{-1/6}\omega^{1/2}C^* \quad (3)$$

Here i_{lim} and i_k are limiting and kinetic currents, n is the number of electrons transferred in the overall electrode reaction, D is the diffusion coefficient, C^* is the solution concentration of O_2, ω is the angular velocity of rotation of an electrode, and ν is the kinematic viscosity of the electrolyte solution. An important mechanistic parameter of the O_2 electroreduction is the number of electrons transferred in the overall process. This allows one to distinguish between the $2e^-$, $2H^+$ pathway leading to H_2O_2 and the $4e^-$, $4H^+$ mechanism in which oxygen is reduced directly to H_2O. These two possible pathways can be distinguished by examining the slope of the Koutecky-Levich plot, which is inversely proportional to n (see Figure 6). The Koutecky-Levich plot shown in Figure 6 is linear and the slope expected for the 3.3 electron reduction, which corresponds to the number of electrons involved in the catalytic reduction of molecular oxygen. The intercept of the plot is expected to be inversely proportional to the rate constant for the current-limiting reaction.[17] Thus, we may expect that the coated catalyst accomplished the reduction of the O_2 to both H_2O_2 and H_2O.

In addition, the rotating ring-disk electrode is commonly employed to differentiate between the $2e^-$, $2H^+$ mechanism and $4e^-$, $4H^+$ mechanisms. As shown in Figure 7, hydrogen peroxide, which is a $2e^-$ reduction product, was confirmed at the ring electrode. The potential of the GC ring electrode was held at 1.0 V *vs.* Ag/AgCl to detect H_2O_2 which was formed on the complex modified disk electrode during the catalytic oxygen reduction process. When the potential of −0.2 V was reached at the disk electrode, the ring current increased immediately. This indicated that the H_2O_2 was detected at the ring electrode as soon as the molecular oxygen

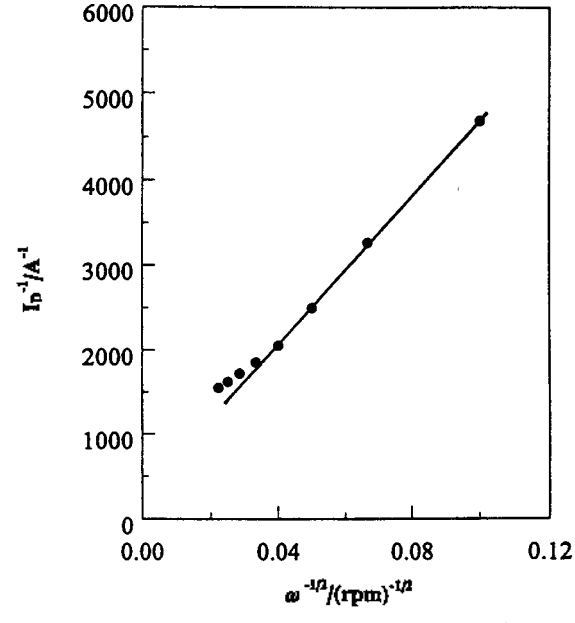

Figure 6. Koutecky-Levich plot of the I_D^{-1} *vs.* $\omega^{-1/2}$. The data was taken from Figure 5.

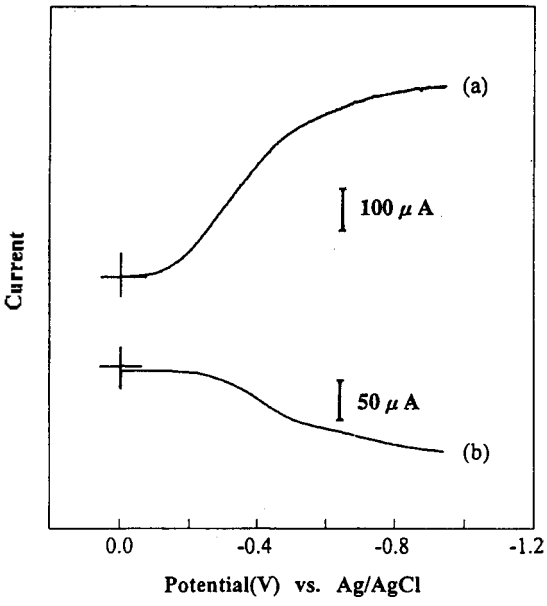

Figure 7. The current-potential curves recorded during the reduction of O_2 for a rotating GC ring-disk electrode in O_2-saturated 0.1 M KNO_3 solution. The GC disk electrode was coated with 1 mM Co(II)-GHA. The potential of the ring electrode was held at 1.0 V *vs.* $Hg/HgSO_4$. The rotation speed was 900 rpm.

was reduced on the disk electrode. A rotating GC ring-disk electrode was also used to determine the relative proportions of the two- and four-electron reductions of oxygen, which occurred on a Co(II)-GHA coated GC disk. In this experiment, the collection efficiency (N) was estimated to be 0.3937 from the geometric factor of the ring and disk electrodes. Theoretically, the N value and the ratio of the ring current (I_R) to the disk current (I_D) should be equal for the two electron reduction reaction of O_2 to H_2O_2. If I_R/I_D is smaller than N, H_2O may be formed *via* the four-electron reduction of O_2 or the decomposition of the H_2O_2.[31] We obtained N=1/2.54 and I_R/I_D=1/4.97, in which the I_R/I_D value was smaller than the N value. From quantitative calculation, the efficiency of O_2 to H_2O_2 through the two electron reduction process was 51%. Thus, the presence of the Co(II)-GHA coated electrode converted 51% of the O_2 to hydrogen peroxide *via* a two-electron reduction pathway, and 49% of O_2 seems to undergo a four-electron reduction to H_2O or degradation reaction of H_2O_2.

The possible reaction pathways for O_2 electrochemical reduction with metal complex coated electrodes in an acid electrolyte are described by the three models which were described by Griffiths,[32] Pauling,[33] and bridged models.[34] Four electron reduction reactions take place in the cases of Griffiths and bridged models, while parallel two and four electrons reductions simultaneously take place in the Pauling model. As described in the previous section, Co-GHA complex modified electrode drives both two and four electron reductions.

Conclusion

The Co(II)-GHA complex coated GC electrode shows electrocatalytic activity for O_2 reduction in aqueous media. With the catalyst coated electrodes, the O_2 reduction potential shifts were 60-510 mV in the positive direction compared to those at the bare GC electrode, depending on the pH. The exchange rate constant value, k_o, was calculated to be 1.27×10^{-7} (cm/sec) at the Co(II)-GHA coated electrode, which was higher than that at the bare GC electrode by about 4 orders. Both two and four electron reductions of O_2 occurred at the Co(II)-GHA complex coated electrode. The interaction between O_2 and Co-GHA complex on the electrode surface should occur with the formation of the M-O-O linkage.

Acknowledgment. This work was supported in part by the Korea Science and Engineering Foundation (the project number: 961-0304-032-2) and by the BSRI program (BSRI-97-3410) of the Ministry of Education of Korea.

References

1. Yeager, E. *Electrochim. Acta.* **1984**, *29*, 1527.
2. Hor, A. M.; Loutfy, R. O.; Hsiao, C. K. *Appl. Phys. Lett.* **1983**, *42*, 165.
3. Zagal, J.; Bindra, P.; Yeager, E. *J. Electrochem. Soc.* **1980**, *127*, 1506.
4. Kobayashi, N.; Fujihira, M.; Sunakawa, K.; Osa, T. *J. Electroanal. Chem.* **1979**, *101*, 269.
5. Ladouceur, M.; Lalande, G.; Dodelet, J. P.; Dignard-Bailey, L.; Tudeau, M. L.; Schulz, R. *J. Electrochem. Soc.* **1993**, *140*, 1974.
6. Brink, V. D. F.; Visscher, W.; Barendrecht, E. *J. Electroanal. Chem.* **1984**, *175*, 279.
7. Zagal, J.; Paez, M.; Tanaka, A. A.; dos Santos, J. R. Jr.; Linkos, C. A. *J. Electroanal.* **1992**, *339*, 13.
8. Galen, V. D. A.; Majda, M. *Anal. Chem.* **1988**, *60*, 1549.
9. Bettelheim, A.; Chan, R. J. H.; Kuwana, T. *J. Electroanal. Chem.* **1979**, *99*, 391.
10. Kuwana, T.; Fujihira, M.; Sunakawa, K.; Osa, T. *J. Electroanal. Chem.* **1978**, *88*, 299.
11. Dong, S.; Liu, B.; Liu, J.; Tabard, A.; Guilard, R. *Electroanalysis* **1995**, *7*, 537.
12. Collman, J. P.; Marrocco, M.; Denisovich, P.; Koval, C.; Anson, F. C. *J. Electroanal. Chem.* **1979**, *101*, 117.
13. Appleby, A. J.; Fleisch, J.; Savy, M. *J. Catal.* **1976**, *44*, 281.
14. Ham, D. V. D.; Hinnen, C.; Magner, G.; Savy, M. *J. Phys. Chem.* **1987**, *91*, 4743.
15. Collman, J. P.; Denisovich, P.; Konai, Y.; Marrocco, M.; Koval, C.; Anson, F. C. *J. Am. Chem. Soc.* **1980**, *103*, 6027.
16. Zhang, J.; Anson, F. C. *J. Electroanal. Chem.* **1993**, *348*, 81.
17. Zhang, J.; Anson, F. C. *J. Electroanal. Chem.* **1992**, *331*, 945.
18. Holdcroft, S.; Funt, B. L. *J. Electroanal. Chem.* **1987**, *225*, 177.
19. Choi, Y. K.; Chjo, K. H.; Park, S. M.; Doddapaneni, N. *J. Electrochem. Soc.* **1995**, *142*, 4107.
20. Basolo, F.; Hoffman, B. M.; Ibers, *Accs. Chem. Res.* **1975**, *8*, 384.
21. Carter, M. J.; Rillema, D. P.; Basolo, F. *J. Am. Chem. Soc.* **1974**, *96*, 392.

22. Tauzher, G.; Amiconi, G.; Antonini, E.; Grunori, M.; Costa, G. *Nature New Biology* **1973**, *241*, 222.
23. Bayer, E. *Chem. Ber.* **1957**, *90*, 2325.
24. Bayer, E. *Angew. Chem. Internat. Edit.* **1964**, *3*, 325.
25. Earnshaw, A.; Hewlett, P. C.; Larkworthy, L. F. *J. Chem. Soc.* **1965**, 4718.
26. Bard, A. J.; Faulkner, L. R. *Electrochemical Methodes*; Wiley: New York, 1990, Chap. 6.
27. Gubbins, K.; Walker, R. *J. Electrochem. Soc.* **1964**, *112*, 469.
28. Costa, G.; Puxeddu, A.; Stefani, L. B. *Inorg. Nucl. Chem. Lett.* **1970**, *6*, 191.
29. Andrieux, C. P.; Saveant, J. M. *J. Electroanal. Chem.* **1982**, *142*, 1.
30. Koutecky, J.; Levich, V. G. *Zh. Fiz. Khim.* **1956**, *32*, 1565.
31. Ohsaka, T.; Watanabe, T.; Kitamura, F.; Oyama, N.; Tokuda, K. *J. Chem. Soc., Chem. Commun.* **1991**, 489.
32. Griffiths, J. S. *Proc. Roy. Soc.* **1956**, *(A) 235*, 23.
33. Pauling, L. *Nature* **1964**, *203*, 182.
34. Collman, J. P.; Denisovich, P.; Konai, Y.; Marrocco, M.; Koval, C.; Anson, F. *J. Am. Chem. Soc.* **1980**, *103*, 6027.

Molecular Dynamics Simulation Studies of Zeolite A. VI. Vibrational Motion of Non-Rigid Zeolite-A Framework

Song Hi Lee* and Sang Gu Choi†

Department of Chemistry, Kyungsung University, Pusan 608-736, Korea
†Department of Industrial Safety, Yangsan Junior College, Yangsan 626-040, Korea
Received October 29, 1997

In the present paper, we report a molecular dynamics (MD) simulation of non-rigid zeolite-A framework only as the base case for a consistent study of the role of intraframework interaction on several zeolite-A systems using the same technique in our previous studies of rigid zeolite-A frameworks. Usual bond stretching, bond angle bending, torsional rotational, and non-bonded Lennard-Jones and electrostatic interactions are considered as intraframework interaction potentials. The comparison of experimental and calculated structural parameters confirms the validity of our MD simulation for zeolite-A framework. The radial distribution functions of non-rigid zeolite-A framework atoms characterize the vibrational motion of the framework atoms. Mean square displacements are all periodic with a short period of 0.08 ps and a slow change in the amplitude of the vibration with a long period of 0.53 ps. The displacement auto-correlation (DAC) and neighbor-correlation (DNC) functions describe the up-and-down motion of the framework atoms from the center of α-cage and the back-and-forth motion on each ring window from the center of each window. The DAC and DNC functions of the framework atoms from the center of α-cage at the 8-ring windows have the same period of the up-and-down motion, but those functions from the center of 8-ring window at the 8-ring windows are of different periods of the back-and-forth motion.

Introduction

The development of accurate, widely applicable, predictive methods for physico-chemical properties estimation based on an understanding of the molecular level processes continues to be an enduring goal for physical chemists. Molecular dynamics (MD) simulation method plays an increasingly important role in understanding the relationship between microscopic interactions and macroscopic physico-chemical properties. This is because MD simulation permits the researcher to selectively switch on and off key intermolecular interactions and evaluate their effect on the property of interest.

There have been a number of applications of MD simulation method to zeolite systems to investigate the local structure and dynamics of adsorbates in zeolite frameworks. For example, Demontis *et al.*, by using simple model potentials, reproduced the positions and vibrations of water molecules in the cages of natrolite,[1,2] the atomic coordinates and the crystal symmetry of dehydrated natrolite[3] and Linde zeolite 4A,[4] and their dynamical behavior in their MD simulation works. Further studies of the group included the diffusive motion of methane in silicate[5] and the structural changes of silicate at different temperatures by a MD method.[6] Cohen de Lara *et al.* also performed a MD study of methane adsorbed in zeolite A[7] based on their potential-energy calculation.[8] Other MD studies on time-dependent properties such as diffusion coefficients and intracrystalline site residence times were reported for methane in zeolite Y,[9] mordenite,[10] and ZSM-5,[10] for benzene in zeolite Y,[11] for water in ferrierite,[12-15] and for xenon,[16] methane, ethane, and propane in silicalite.[17] The dynamics of Na^+ ions inside a

*To whom correspondence should be addressed.